Front. Optoelectron. China 2010, 3(1): 2–8
DOI 10.1007/s12200-009-0087-8

REVIEW ARTICLE

What do you see in photonic crystal fibers?

Jonathan C. KNIGHT (✉)

Centre for Photonics and Photonic Materials and Department of Physics, University of Bath, Bath BA2 7AY, UK

Abstract Photonic crystal fibers have been a source of colorful and intriguing optical images from the time they were first developed. The images are all the more captivating because they often transmit information about the basic optical properties of the fiber—sometimes in a visually spectacular way. Some of the more significant effects that are apparent in this way are demonstrated, along with an interpretation of their meaning.

Keywords optical fiber, nonlinear fiber optics, photonic crystal fibers, supercontinuum

1 Introduction

There is something special about working in optics or photonics in that it allows one to actually see new effects with one's own eyes. This sets it apart from most other branches of physics or engineering, wherein effects have to be observed or represented through graphs, oscilloscope traces, or numbers. In the field of photonic crystal fibers (PCFs), this has been especially valuable because the recorded visual images have been scientifically informative while simultaneously being colorful and intriguing. Thus, many of the most spectacular advances—the first PCF and the first air-core fibers, for example, or visible supercontinuum generation—became genuine "Eureka" moments, requiring little or no analysis to establish beyond doubt that some new (or just newly spectacular) physical phenomenon has been observed. The excitement that this has generated has undoubtedly contributed to the "Woodstock" feeling of many of those working in this field over the last decade. This has not only enabled young scientists to work in an exciting area with genuine possibilities of seeing new effects for themselves but has also ensured that a new generation of scientists have become more familiar with the remarkable body of work done in developing optical fibers since the early 1970s. It would require a book, not just a paper, to describe the effects that have been "discovered" using PCFs but that were first reported in the remarkable early years of optical fiber development. However, that is not the intention here. Rather, the purpose of this paper is to enable researchers, especially experimentalists, to gain insight into the behavior of PCFs on the basis of what they can see with their own eyes and with the help of a camera or microscope. The paper is divided into several sections. Following this introduction, Sect. 2 describes the actual fibers used in the experiments to be described. Many of the images to be discussed were recorded using light leaving the end of the fiber, as it properly should. Near-field and far-field patterns are the subjects of Sects. 3 and 4. Section 5 describes some effects that can be observed by observing light which has left the fiber through the side walls and never made it to the far end of the fiber and is thus "lost". It should be said that the effects described here are not intended to be all those that can be observed but a subset that show striking effects while offering some physical insight and opportunity for thought.

Received August 1, 2009; accepted November 19, 2009

E-mail: j.c.knight@bath.ac.uk

2 PCF structures

Since coming into the limelight in the mid-1990s [1,2] PCFs have been widely investigated both experimentally and theoretically and by now are the subject of a massive scientific literature. For a comprehensive understanding of the topic, the reader is referred to one of the reviews or books on the subject. The purpose of this section of the present work is simply to provide the details of the types of fibers used in the remainder of the paper.

The different fiber structures used are shown in Fig. 1. They are all formed from silica, doped silica, and air. The actual fibers used differ from those shown in Fig. 1 only in size scale and detail. The fibers guide light by modified total internal reflection (Figs. 1(a) and 1(b)) [2] and by a photonic band gap [1,3,4] (Figs. 1(c) and 1(d)). The fiber shown in Fig. 1(a) is an endlessly single-mode fiber, with a solid pure silica core surrounded by an array of relatively

small air holes. Figure 1(b) shows a fiber that also guides by total internal reflection, but now the air holes are larger. As a result, the fiber guides more than a single mode. The larger air holes also result in stronger waveguide dispersion for the fundamental mode [5], and this fiber has several advantages for supercontinuum generation [5,6]. The fibers shown in Figs. 1(c)–1(e) are different forms of photonic band-gap fiber. In the first case, the core is hollow [3,7], while, in the second [4] and third [8] cases, which are very similar to one another, the core is formed from undoped silica, but the cladding has an array of raised-index elements. In all three cases, the core-guided modes are formed within gaps in the density of photonic states in the cladding, and the effective index of the core modes is below the highest effective index of modes in the cladding. In all band-gap fibers, the core-guided modes are only confined over limited spectral ranges.

3 Cladding modes: near-field patterns

Understanding the cladding modes in photonic crystal and microstructure fibers is essential to understand and predict the existence and properties of core-guided modes; therefore, observing the cladding modes is a worthwhile pursuit in its own right. Most commonly, a wide variety of cladding mode structures—individual cladding modes or superpositions of modes—can be easily observed using a simple optical microscope. Generally, when using a microscope to study PCF, illuminating the sample from above (e.g., through the microscope objective) means that the image is built up of light, which is scattered and reflected at the top (cleaved) surface of the fiber. Consequently, the image is built from a continuum of plane waves incident on the imaged sample end-face, and the image should be broadly representative of the morphological structure of the fiber, albeit with limited resolution. In contrast, if a length of fiber is used (perhaps a few millimeters or centimeters) and the illumination is at the far end, then the image can only be formed using the modes supported by the fiber cladding. In this case, the image that one sees can differ significantly from that observed when using reflected light, and measuring parameters of the fiber structure from this image can give completely incorrect results. On the other hand, the "transmitted light" images offer insight into the nature of the modes guided in the fiber. Thus, reflected light images contain more and better direct information about the structure itself, with transmitted-light images being more representative of fiber mode patterns than of the actual fiber microstructure.

The spatial patterns of the cladding modes of PCFs are usually (but not always!) concentrated in the high-index regions of the structures. They are also frequently periodic, taking on the period of the fiber microstructure. A commonly asked question is whether the photonic band gap that confines the light in a hollow-core photonic band-gap fibers guide light by Bragg reflection, anti-resonant reflection, or some other mechanism. An anti-resonant reflection optical waveguide (ARROW) model has been shown to be an excellent model that can quantitatively explain many features of photonic band-gap fibers with all-solid claddings [9]. In the ARROW model, the non-guiding wavelengths are determined by the cutoffs of the guided modes of the individual guiding (high-index) elements in the cladding structure. In the case of

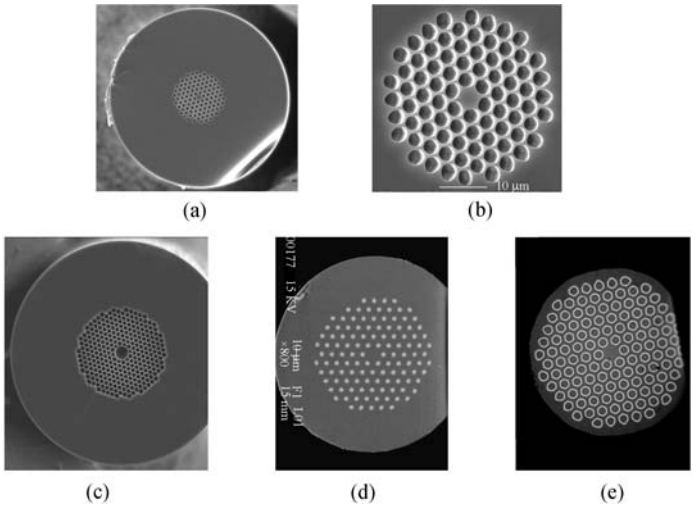

Fig. 1 Scanning electron micrographs of fiber designs discussed in this paper. (a) Single-mode solid-core PCF; (b) high-Δ solid-core PCF; (c) hollow-core photonic band-gap fiber; (d) all-solid photonic band-gap fiber; (e) all-solid band-gap fiber based on rings in the cladding

hollow-core fiber, the cladding is necessarily formed of a self-supporting lattice of webs and strands of glass, and the modes supported are complex. However, in all-solid band-gap fibers, the modes are well approximated by those of single waveguides. Thus, the modes in the cladding can be readily identified with the modes of individual circular waveguides.

Examples are shown in Fig. 2. The images are of the output face of an all-solid photonic band-gap fiber in which the high-index inclusions in the cladding are in the forms of rings of doped silica embedded in a pure silica background [8]. They show how the modal field patterns observed in the cladding can be used to unambiguously identify specific modes in the fiber cladding. A further example is shown in Fig. 3, recorded from a somewhat different fiber in which the high-index cladding inclusions are simply circular disks in cross-section [10]. Here, the cladding patterns show different radial modes of the high-index inclusions as well as the azimuthal modes in Fig. 2. As shown in Ref. [8], the azimuthal modes are suppressed in the ring fiber structure. In Fig. 3, observing the variation of cladding modes with wavelength, along with the computed mode patterns, enables unambiguous identification of the order of various band gaps.

4 Far-field patterns

Light leaving the core of an optical fiber in single-mode diffracts into free space (in the absence of any intervening optics) and after propagating a suitable distance—typically from a few tens of microns to a few millimeters [11]—forms a stable pattern, the far-field pattern, which corresponds to the Fourier transform of the pattern in the near field. The far-field pattern is often the first pattern one see when coupling light into a new fiber, if that is being done at visible frequencies on an optical bench rather than under a microscope. As such, the more one can learn from it the better. In a single-mode fiber, the far-field pattern remains constant when the input coupling is varied, varying only in intensity. If the fiber guides more than a single mode, one can usually observe several different field patterns as the excitation condition is changed. A far-field pattern recorded by exciting the guided mode in an endlessly single-mode fiber as shown in Fig. 1(a) using a broadband supercontinuum source [12] is shown in Fig. 4(a). The input spectrum contains all visible wavelengths, and the fiber design ensures that this wide range of wavelengths all propagate single-mode to the fiber output end. When they leave the end of the fiber, they form a pattern that is determined by the near-field pattern [2], which clearly demonstrates the confining nature of the air holes. The central part of the far-field pattern is white to the eye because all of the wavelengths in the transmitted spectrum are roughly equally represented there (in reality, the central part of the image shown in Fig. 4(a) is saturated on the cameras charge-coupled device (CCD)). However, at the edges, bright colors appear, as a result of the fact that the size of the guided mode is roughly constant with wavelength, so that the numerical aperture (NA) scales with the wavelength [13].

Visible supercontinuum generation has produced a series of striking images since it was first observed in PCF in 2000 [5]. One way in which supercontinuum spectra can be extended to shorter wavelengths is by using higher-order modes—either by exciting these modes at the fundamental (pump) wavelength (see, e.g., Ref. [14]) and making use of the fact that the dispersion curves for these modes are very different to those of the fundamental mode (for the same core size) or by exciting the fundamental mode at the pump wavelength but using modal phase-matching to couple energy into the higher modes at specific wavelengths, typically through modally phase-matched third-harmonic generation [15]. Figures 4(b) and 4(c) show far-field patterns observed by exciting a supercontinuum in a silica fiber. Both images were recorded by exciting a birefringent nonlinear fiber [16] using a pulse train from a mode-locked TiSapph laser system. The elliptical core made it easy to simultaneously excite more than the fundamental mode of the fiber. In this

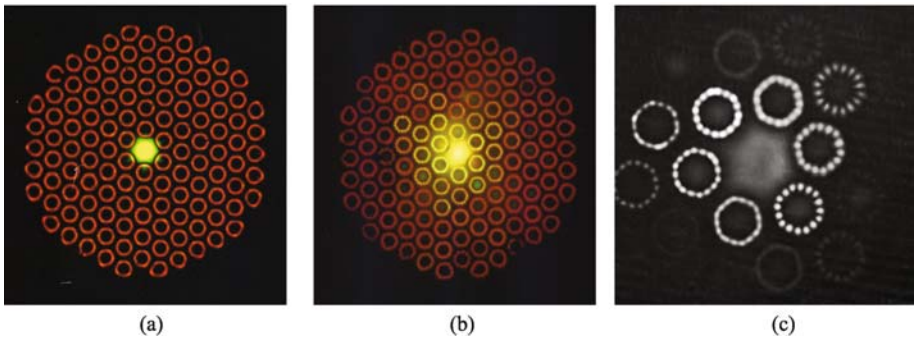

Fig. 2 Images of near-field intensity patterns observed using ring-cladding band-gap fiber [8]. (a) Image recorded using conventional microscope in transmission, showing core-guided mode; (b) similar image but with excitation adjusted to demonstrate excitation of some cladding modes; (c) image recorded using an imaging objective lens demonstrating specific mode being excited in cladding rings

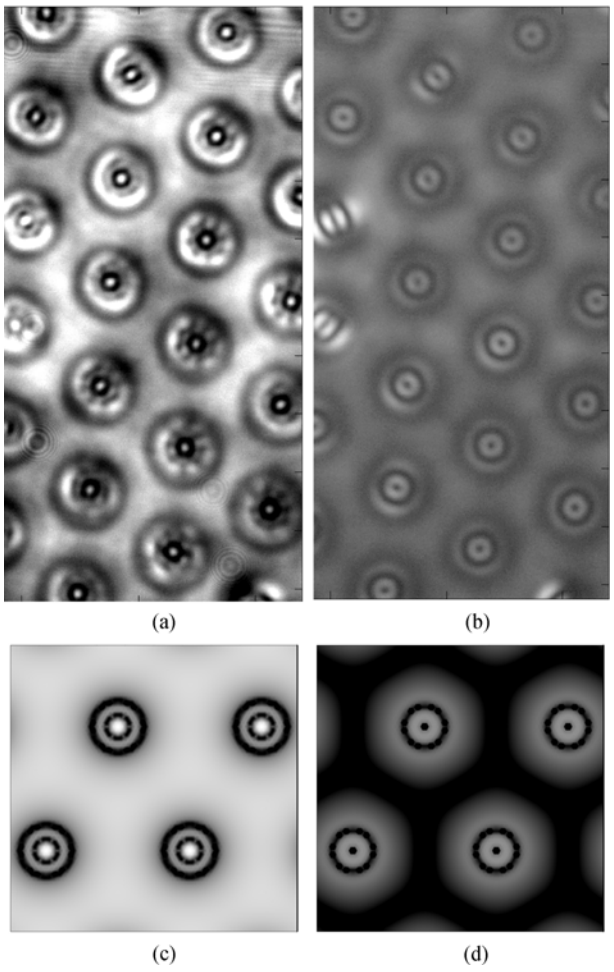

Fig. 3 Modal field patterns recorded in cladding of all-solid photonic band-gap fiber. (a) At 896 nm; (b) at 1007 nm; (c) corresponding computed field patterns at 896 nm; (d) corresponding computed field patterns at 1007 nm [10]

case, the resulting nonlinear processes were sensitive to the polarization state of the pump light, and the two different output patterns correspond to rotation of the incident polarization vector with no other changes.

5 Scattered light

Of the light coupled into one end of an optical fiber, only some leaves at the far end. Some of the remainder is lost through the sides of the fiber along the length, either due to confinement loss, through bend loss, or through scattering. In photonic band-gap fibers, this light is especially interesting because, in order to leave through the fiber walls, the light must pass through the fiber cladding—through the photonic band-gap material. Considering the range of angle at which light could leave the fiber, light that travels at an angle approaching parallel to the fiber axis in the air outside of the fiber will be propagating at a larger angle in the jacketing material or in the photonic band-gap cladding. However, it will be at the same angle in the fiber core, which is also made of air. Thus, the light that is trapped in the core-guided mode of the fiber is also able to propagate in free space outside of the fiber. This is not the case with index-guided fibers, in which the propagation constant of the core-guided modes is higher than the largest value of the propagation constant, which can propagate in free space. The result is that we can hope to identify the features of the photonic band-gap cladding by studying the light escaping through the fiber walls. Measurements based on side-scattered light have been used to map out the photonic band gap and identify individual modes in a hollow-core fiber operating at 1550 nm. However, we show here how the photonic band gap in such fibers can be directly observed, with the unaided eye, in fiber designed to operate at visible wavelengths.

The images shown in Fig. 5 show a hollow-core fiber designed to guide light at visible frequencies. Light introduced at the far end of the fiber is propagating along the fiber towards the camera. The fiber is laid flat and straight on an optical bench (see Fig. 5(a)). With the room lights off (Fig. 5(b)), the far end of the fiber is dark, while the front end, closer to the camera, is bright. As the camera is lowered, the point along the fiber where it goes from bright to dark moves along the fiber as the angle subtended by the camera at the fiber alters (Fig. 5(c)). This transition

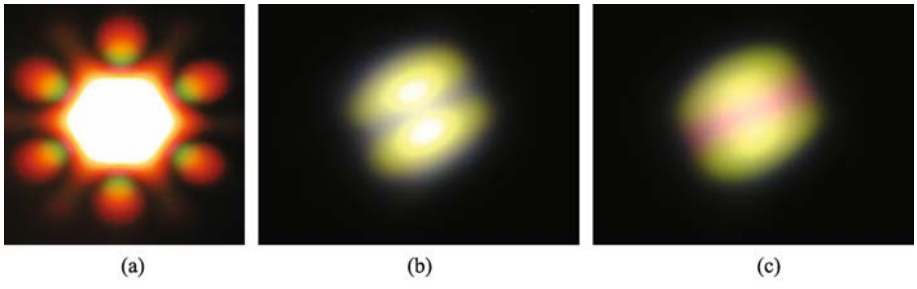

Fig. 4 Far-field images recorded using supercontinuum generated in a PCF. (a) Supercontinuum spectrum generated using sub-nanosecond pulses at 1.06 μm and an endlessly single-mode supercontinuum fiber [12] (white light in the center of the far-field pattern gives way to colors at the edges due to the variation in numerical aperture with wavelength [13]); (b) and (c) supercontinuum generated simultaneously in both fundamental and higher modes of a highly birefringent PCF (different colors shown in (b) and (c) were generated using different input polarization states)

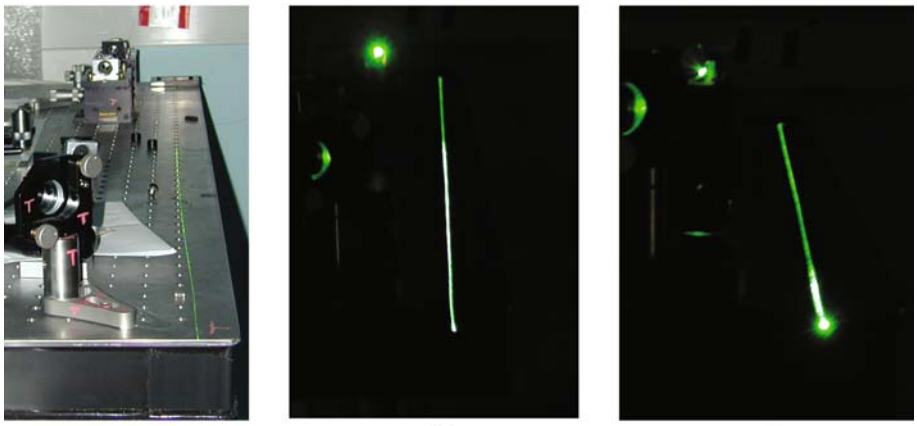

Fig. 5 Side-scattering method of visualizing band gap in a hollow-core band-gap fiber. (a) Experimental configuration (green-guiding hollow-core fiber is laid out on the optical bench; green light is coupled into the core at the far end of the bench, propagating towards the camera); (b) with the room lights off, it is apparent that the far end of the fiber is significantly darker than the near end; (c) when the camera is lowered, the point at which the fiber becomes dark moves towards the camera, indicating that it is determined by the angle relative to the fiber axis (angle corresponds to the edge of the band gap in the fiber cladding)

point corresponds to the edge of the photonic band gap, which is trapping light in the core. Those angles corresponding to the fiber being dark lie within the band gap. Indeed, this means that, with a simple ruler and one's eye, one can readily calculate the propagation constant and effective index at the edge of the photonic band gap in the fiber at the wavelength being used. The effect observed described here was studied more fully in Ref. [17] in which the fiber was immersed in index-matching fluid to enable access to the entire photonic band gap rather than just the band-gap edge.

If a supercontinuum source is used with a similar fiber, spectacular effects can be seen at low angles due to the variation of the effective index with wavelength and the leakage of light close to the band-gap edge. An illustration is shown in Fig. 6, which shows a fiber designed to guide green light laid in loops on the optical bench, with the light in the loops travelling towards the camera. At most points along the fiber, the light entering the camera lens has left the fiber at a relatively large angle with respect to the fiber axis. Seeing the angles concerned do not lie within the numerical aperture of the input objective lens; this light must have been scattered in transiting the optical cladding of the fiber or the polymer coating material. No matter the wavelength, this light does not lie within the photonic band gap because the propagation constant in the fiber is too low. The overall appearance of the visible portion of the spectrum leaving the fiber along most of the length thus broadly matches that of the input light source. As one moves along the fiber (downwards in the image), the angle of the light forming the image on the camera CCD decreases as the fiber swings to point more directly at the camera. When this angle approaches the minimum, there are dramatic changes in both the spectral content of the light coming from the fiber and its brightness. First, as the angle decreases the intensity drops and the color takes on a bright-green coloration, the orange and yellow light can no longer leave the core as it now falls within the photonic band gap. When the angle is decreased further, the band gap extends to higher frequencies, and the green light is unable to transit the fiber axis as well. At this point, the intensity of light leaving the fiber is at a minimum and the color is reddish. Orange, yellow, and green light is unable to leave the fiber core and is trapped by the cladding band gap. Yet shorter wavelengths that may have been present in the original input spectrum are not visible at this point because they were more strongly attenuated due to leakage and scattering immediately after being coupled into the fiber and are only weakly present at this point along the fiber length.

Fig. 6 Green-guiding hollow-core photonic band-gap fiber excited using a broadband supercontinuum source (bright colors visible when the fiber is most close to directly approaching the camera are a result of the dependence of the band-gap edge on angle and wavelength)

Light that never reaches the output end of the fiber can help understand aspects of supercontinuum generation as well. An example is shown in Fig. 7, in which two identical pump sources are simultaneously exciting two different supercontinuum fibers. In the case shown, the two fibers differ only in the size of their air holes [6]. However, the spectra generated are visibly different, with the fiber closer to the camera generating shorter wavelengths than the other. As a result, the light scattered through the side of the supercontinuum fiber has a significantly whiter look as a result of the increased blue components in the spectrum.

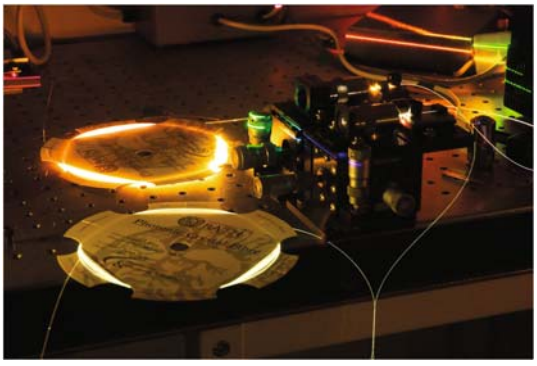

Fig. 7 Two identical pump lasers are used to pump two very similar supercontinuum fibers. The difference between the fibers is in the size of the air holes: the core sizes are the same. Due to group-index matching effects [6], the supercontinuum in the fiber with the larger holes extends significantly further to shorter wavelengths, giving a whiter appearance to the side-scattered light

A way to generate even shorter wavelengths is the use of a nonlinear fiber that tapers along its length [18]. Clearly, designing such a fiber profile is a highly complex inverse problem, but some indication of what is required can be obtained from simple thinking. If one wants to convert the maximum energy to shorter wavelengths than the pump, then the fiber at the input end should be designed to spread the spectrum as symmetrically as possible. That means that the input fiber should favor modulation instability or four-wave mixing, implying that the fiber dispersion should be low or zero at the pump wavelength. Strong and broadband anomalous dispersion would result in multiple soliton generation, and the subsequent Raman self-scattering would result in more of the pump energy being shifted to longer rather than shorter wavelengths. Typically, pump sources are in the wavelength range around 800 to 1060 nm, and this implies a fiber core size of around 3 to 5.5 μm. On the other hand, to generate the shortest possible wavelengths, it is beneficial to taper the fiber to a smaller core size along its length, for several reasons. One is simply that it increases the nonlinear coefficient. A second reason is that it will cause group-index matching between the long and the short edges of the supercontinuum to occur for shorter wavelengths than for the larger core. A third reason is that it causes a reduction in anomalous dispersion at long wavelengths, compressing the solitons in that spectral range and causing them to shift faster to longer wavelengths, simultaneously increasing the blue component of the supercontinuum. In using such a tapered fiber, we have sometimes observed an angle-dependent leakage from the fiber near to the output (small) end of the taper, as illustrated in Fig. 8. The shortest wavelengths are emitted at the smallest angles, while longer wavelengths appear at larger angles to the fiber axis, up to perhaps 30°. At even larger angles, the fiber is relatively dark. This is a very striking effect, not unlike that shown in Fig. 5, but possibly with different underlying physics. The effect is not observed in all the tapers, and the origin remains unclear.

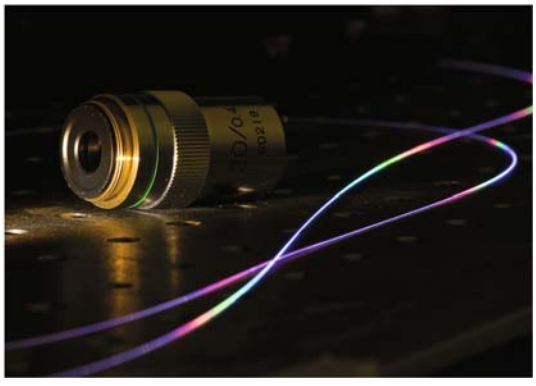

Fig. 8 Tapered supercontinuum fiber used to generate ultraviolet wavelengths using either sub-nanosecond or sub-picosecond pulses from *Q*-switched or mode-locked 1 μm pump sources [18]. In some cases, the tapered fiber results in spectral leakage through the side of the fiber. The origin of this effect is yet to be determined

6 Conclusion

PCFs offer some visually spectacular effects, not only providing great opportunities for photography and promotion but also enabling valuable insight into the physical mechanisms at work. The examples described here are just a few of those that we have come across over the last few years in our laboratories, and we hope that this paper will stimulate students and others to look at their work critically in an effort to understand what they are seeing.

Acknowledgements The author would like to acknowledge the contribution made to this paper by many of his colleagues and former colleagues at the University of Bath.

References

1. Birks T A, Roberts P J, Russell P St J, Atkin D M, Shepherd T J. Full 2-D photonic bandgaps in silica/air structures. Electronics Letters,

1995, 31(22): 1941–1943

2. Knight J C, Birks T A, Russell P St J, Atkin D M. All-silica single-mode optical fiber with photonic crystal cladding. Optics Letters, 1996, 21(19): 1547–1549
3. Cregan R F, Mangan B J, Knight J C, Birks T A, Russell P St J, Roberts P J, Allan D C. Single-mode photonic band gap guidance of light in air. Science, 1999, 285(5433): 1537–1539
4. Luan F, George A K, Hedley T D, Pearce G J, Bird D M, Knight J C, Russell P St J. All-solid photonic bandgap fiber. Optics Letters, 2004, 29(20): 2369–2371
5. Ranka J K, Windeler R S, Stentz A J. Visible continuum generation in air-silica microstructure optical fibers with anomalous dispersion at 800 nm. Optics Letters, 2000, 25(1): 25–27
6. Stone J M, Knight J C. Visibly "white" light generation in uniform photonic crystal fiber using a microchip laser. Optics Express, 2008, 16(4): 2670–2675
7. Allan D C, Borelli N F, Gallagher M T, Muller D, Smith C M, Venkataraman N, West J A, Zhang P H, Koch K W. Surface modes, loss in air-core photonic band-gap fibers. In: Proceedings of the Society of Photo-Optical Instrumentation Engineers. 2003, 5000: 161–174
8. Stone J M, Pearce G J, Luan F, Birks T A, Knight J C, George A K, Bird D M. An improved photonic bandgap fiber based on an array of rings. Optics Express, 2006, 14(13): 6291–6296
9. Litchinitser N M, Dunn S C, Usner B, Eggleton B J, White T P, McPhedran R C, de Sterke C M. Resonances in microstructured optical waveguides. Optics Express, 2003, 11(10): 1243–1251
10. Birks T A, Luan F, Pearce G J, Wang A, Knight J C, Bird D M. Bend loss in all-solid bandgap fibres. Optics Express, 2006, 14(12): 5688–5698
11. Mortensen N A, Folkenberg J R. Near-field to far-field transition of photonic crystal fibers: symmetries and interference phenomena. Optics Express, 2002, 10(11): 475–481
12. Wadsworth W J, Joly N, Knight J C, Birks T A, Biancalana F, Russell P St J. Supercontinuum and four-wave mixing with Q-switched pulses in endlessly single-mode photonic crystal fibres. Optics Express, 2004, 12(2): 299–309
13. Gander M J, McBride R, Jones J D C, Birks T A, Knight J C, Russell P St J, Blanchard P M, Burnett J G, Greenaway A H. Measurement of the wavelength dependence of beam divergence for photonic crystal fiber. Optics Letters, 1999, 24(15): 1017–1019
14. Cherif R, Zhgal M, Tartara L, Degiorgio V. Supercontinuum generation by higher-order mode excitation in a photonic crystal fiber. Optics Express, 2008, 16(3): 2147–2152
15. Omenetto F G, Taylor A J, Moores M D, Arriaga J, Knight J C, Wadsworth W J, Russell P St J. Simultaneous generation of spectrally distinct third harmonics in a photonic crystal fiber. Optics Letters, 2001, 26(15): 1158–1160
16. Ortigosa-Blanch A, Knight J C, Wadsworth W J, Arriaga J, Mangan B J, Birks T A, Russell P St J. Highly birefringent photonic crystal fibers. Optics Letters, 2000, 25(18): 1325–1327
17. Couny F, Sabert H, Roberts P J, Williams D P, Tomlinson A, Mangan B J, Farr L, Knight J C, Birks T A, Russell P St J. Visualizing the photonic band gap in hollow core photonic crystal fibers. Optics Express, 2005, 13(2): 558–563
18. Kudlinski A, George A K, Knight J C, Travers J C, Rulkov A B, Popov S V, Taylor J R. Zero-dispersion wavelength decreasing photonic crystal fibers for ultraviolet-extended supercontinuum generation. Optics Express, 2006, 14(12): 5715–5722